Indian Journal of Chemistry
Vol. 65, May 2026, pp. 426-438
DOI: 10.56042/ijc.v65i5.20786

Computational investigation of selected flavonoids as caspase-3 inducers in multidrug-resistant leukemia

Dung Manh Ngo & Hung Duc Nguyen*
Thai Nguyen University of Education, 24000, Thai Nguyen, Vietnam
E-mail: hungnd@tnue.edu.vn

Received 18 June 2025; accepted (revised) 14 May 2026

Leukemia is one of the most common forms of cancer worldwide, particularly in children. Multidrug-resistant leukemia remains a significant challenge in cancer therapy due to resistance mechanisms, including drug efflux pumps. Apoptosis, particularly *via* caspase-3 activation, is a key target to overcome this resistance. This study aims to explore and assess the mechanisms of flavonoids CPD5, CPD7, and doxorubicin as potential agents against multidrug-resistant leukemia. Key molecular targets identified include JNK1, AKT1, MAPK3, TP53, NFKB1, and CREB1, linked to apoptosis signaling. Molecular docking with the caspase-3 structure (PDB ID: 4JJE) reveals that CPD5 and doxorubicin exhibit more stable binding energies and better localization within the protein 4JJE compared to CPD7. Molecular dynamics simulation over 100 ns confirms stable binding interactions for all compounds. *In silico* ADMET predictions have assessed oral bioavailability, showing CPD7 meets all pharmacokinetic criteria, being non-toxic, with superior distribution capacity and high absorption. These findings suggest CPD7 as a promising future drug for treating multidrug-resistant leukemia by inducing apoptosis through caspase-3 activation.

Keywords: ADMET, apoptosis, caspase-3, flavonoids, multidrug-resistant leukemia

Multidrug resistance (MDR) is a primary mechanism by which cells, including bacteria and cancer cells, become resistant to multiple types of drugs. This resistance is often attributed to the overexpression of drug efflux pumps, which are proteins that transport drugs out of the cell[1,2]. Significant research efforts are focused on developing and implementing strategies to reduce leukemia risk and improve treatment outcomes. This includes focusing on lifestyle modifications, addressing environmental exposures, and developing new therapeutic approaches[3]. Chemotherapy continues to be the primary treatment approach for leukemia patients, as per current medical practice[4]. Up to date, conventional chemotherapy involves using drugs to destroy cancer cells by targeting their rapid growth and division, though it can also harm healthy cells. This systemic treatment is delivered through the bloodstream to reach cancer cells throughout the body, even those that have spread. It is a primary treatment option, but side effects and limitations like resistance and targeting cancer stem cells are being addressed with new approaches. Apoptosis, or programmed cell death, is a significant therapeutic target in cancer treatment, particularly due to its potential to induce cancer cell death and overcome chemotherapy resistance. By targeting and activating apoptotic pathways, researchers aim to eliminate cancer cells, leading to improved therapeutic outcomes[5]. Caspase-3 is a critical enzyme in the apoptotic pathway, which acts as an executioner caspase, cleaving various cellular proteins to dismantle cellular components during apoptosis[6].

Plant-derived compounds have been crucial in developing effective cancer treatments, with many current chemotherapy drugs originating from plants. These drugs target various cellular processes crucial for cancer cell growth and division, such as cell cycle regulation, DNA replication, and apoptosis[7]. Plant-derived compounds are receiving increased global attention from researchers due to their potential in drug discovery and addressing various health challenges, including antibiotic resistance and cancer treatment[8]. Meanwhile, flavonoids, a class of naturally occurring polyphenols, have shown considerable promise in cancer prevention and treatment due to their diverse anticancer properties. They inhibit cancer cell growth, promote apoptosis, and modulate various signaling pathways in cancer development[9]. Previous studies of our colleagues have

led to the identification of two potential flavonoids from *Platycodon grandiflorus* (Jacq.) A. DC. And *Dracaena steudneri* Eng. with cytotoxicity against leukemia cell lines, but their mechanism are still unexplored[10]. This led us to carry out this study to discover and evaluate the mechanism of these flavonoids using multiple computational techniques. Molecular docking, molecular dynamics simulation, and ADMET predictions were carried out with the aid of molecular target predictions to identify key interactions, particularly with caspase-3. The findings provide a foundation for future experimental validation and optimization of these flavonoids as effective and safe treatments for leukemia cancer, pending further *in vitro* and *in vivo* studies.

Experimental Section

Collection and Preparation of Ligands

The flavonoids possessing cytotoxic activity against leukemia cancer cell lines (CEM/ADR5000) were collected through literature source[10]. For details, these ligands, including 3,3'-di-*O*-methylquercetin-4'-*O*-β-D-glucoside (CPD5) and 3,3'-di-*O*-methylquercetin (CPD7), have molecular formulas of $C_{23}H_{24}O_{12}$, $C_{17}H_{14}O_7$, and molecular weights of 492.1268, 330.074 Da, respectively (Fig. 1). The 2D structures of ligands were prepared in .sdf format using ChemDraw Prime v23.1 (Perkin Elmer, USA) and converted to 3D structures in .pdb format using Biovia Discovery Studio Visualizer v24.1 (Dassault Systemes BIOVIA, USA). Polar hydrogens and Gasteiger charges were also added, and all torsion angles were allowed to rotate using AutoDock Tools 1.5.7 (Center for Computational Structural Biology, USA). The 2D structure of Doxorubicin (molecular formula of $C_{27}H_{29}NO_{11}$ and molecular weight of 543.1741 Da*)* was obtained from the PubChem database in .sdf format (https://pubchem.ncbi.nlm.nih.gov) and further converted to .pdb format using Biovia Discovery Studio Visualizer (Fig. 1).

Selection and Preparation of Macromolecule

The 3D conformation of target caspase-3 (protein ID: 4JJE) was retrieved from RCSB Protein Data Bank (https://www.rcsb.org/) in .pdb format[11]. The preparation process involved preparing receptors and removing water molecules using Biovia Discovery Studio Visualizer. Appropriate binding orientations and conformations of the ligand molecules with protein inhibitors were performed using AutoDock Tools. All co-crystalized ligands were cut from the protein complexes and used to validate the molecular docking protocol by calculating root mean square deviation (RMSD) using Biovia Discovery Studio Visualizer. After the protein was cleaned, only polar hydrogens and the Kollman charges were introduced.

Molecular target prediction

The 2D structure between each drug and the ligand set of each target was measured as an expectation value (E-value) through the Similarity Ensemble Approach (SEA)[12]. The SMILES strings for both selected flavonoids were obtained and entered into the SEA database (http://sea.bkslab.org), with *Homo sapiens* specified as the target organism to ensure predictions relevant to humans. The SEA platform generated a ranked list of potential protein targets based on statistical significance, which were then mapped to known metabolic and signaling pathways using resources such as KEGG and UniProt. This approach facilitated identifying biological processes potentially affected by the selected flavonoids, providing a foundation for further investigation into their mechanisms of action.

Protein-protein interaction network prediction

The protein-protein interaction (PPI) networks associated with the selected flavonoids were analyzed using the STRING database (https://string-db.org), a reliable tool for exploring known and predicted protein interactions[13]. The potential target proteins identified from the SEA analysis were entered into

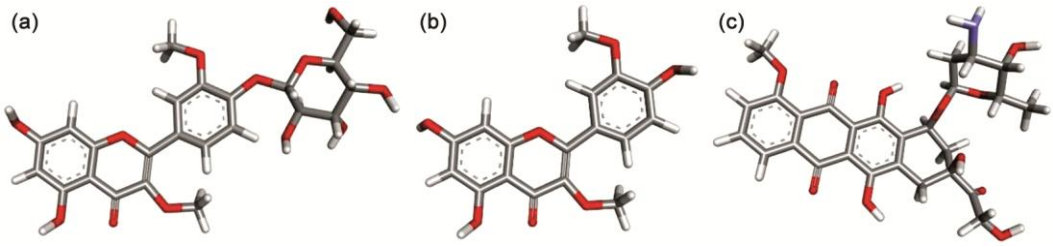

Fig. 1 — 3D structure of the selected ligands. (A) 3,3'-di-*O*-methylquercetin-4'-*O*-β-D-glucoside (CPD5), (B) 3,3'-di-*O*-methylquercetin (CPD7) and (C) the comparative ligand, Doxorubicin.

STRING, with *Homo sapiens* specified as the reference organism to ensure human biological relevance. The generated PPI network provided critical insights into the potential interactions among the predicted flavonoid targets and their links to other key regulatory proteins involved in cell signaling, apoptosis, and metabolic pathways. These networks are essential for understanding the compounds' potential mechanisms of action from a systems biology perspective.

Biosignaling network prediction

Biosignal network prediction uses machine learning, particularly neural networks, to analyze physiological data and predict health outcomes, enabling early disease detection and improved treatment planning. The X2K Web platform (https://maayanlab.cloud/X2K/) was used to explore upstream regulatory networks of flavonoid target proteins, integrating predictive insights with molecular pathway analysis[14]. X2K combines transcription factor, kinase, and protein-protein interaction analyses to generate regulatory networks for input gene sets from SEA and STRING, with *Homo sapiens* as the reference species. The resulting network, including transcription factors, adaptor proteins, and kinases, revealed how flavonoids may regulate gene expression and signaling pathways in human systems.

Molecular docking

Polar hydrogens and Gasteiger charges were added, and all torsions were allowed to rotate using AutoDock Tools. A 3D grid was generated using the AUTOGRID algorithm, defining a box grid to measure the binding energy of ligands with the receptor. The grid dimensions were set to $x = 64$, $y = 52$, $z = 52$, with a spacing of 0.375 Å between grid points. The docking site coordinates were identified as $x = 39.726$ Å, $y = 12.854$ Å, and $z = 68.864$ Å within the 4JJE protein pocket. The Lamarckian genetic algorithm determined the most energetically favorable ligand-protein binding conformations[15].

Molecular dynamics simulation

The protocol to carry out molecular dynamics simulation is detailed in a previous study[15]. For specifics, a 100 ns molecular dynamics simulation was executed for the optimal docked conformation of the 4JJE protein using GROMACS v2024.4 using the CHARMM36 force field[16]. The protein structure was corrected with Swiss-PdbViewer to address missing atoms and residues[17]. Ligand topologies were created using Swiss PARAM[18]. The protein-ligand complex was solvated in a triclinic box with the SPC water model, supplemented by 0.15 M sodium chloride. Structural optimization involved energy minimization and neutralization over 50,000 steps. The system was stabilized at 300 K in a 100 ps constant-volume simulation with a 1 fs time step. Subsequently, a 2 fs time step was used in a 100 ps NPT simulation to adjust the pressure to 1 atm. Data from the simulation were processed at 100 ns with UCSF Chimera v1.17.3 and Grace software[19], evaluating root mean square deviation (RMSD), per-residue root mean square fluctuation (RMSF), radius of gyration (Rg), and the count of hydrogen bonds (H-bonds) per frame over time.

***In silico* evaluation of pharmacokinetic parameters**

In silico evaluation using pkCSM (Predicting Kinetics and Small Molecule characteristics) is a computational approach to estimate pharmacokinetic parameters of small molecules, including absorption, distribution, metabolism, excretion, and toxicity (ADMET). It uses algorithms to predict these properties based on the molecule's chemical structure, helping researchers in drug discovery and development. Therefore, the drug-likeness properties of selected compounds were evaluated using the pkCSM databases[20].

Results and Discussion

Molecular target, protein interaction, and biosignaling network

According to the molecular target predictions listed in Table 1, the seleted flavonoids have been associated with several key human targets, notably P-glycoprotein (ABCB1), broad substrate specificity ATP-binding cassette transporter ABCG2 (ABCG2), multidrug resistance-associated protein 1 (ABCC1), protein disulfide-isomerase (P4HB), cytochrome P450 1B1 (CYP1B1), xanthine dehydrogenase/oxidase (XDH), NADPH oxidase 4 (NOX4), death-associated protein kinase 1 (DAPK1), arachidonate 5-lipoxygenase (ALOX5), ribosomal protein S6 kinase alpha-3 (RPS6KA3), cyclic AMP-responsive element-binding protein 1 (CREB1), and DNA topoisomerase 2-alpha (TOP2A), among others. Notably, ABCB1 emerged as a pivotal protein connecting drug resistance mechanisms in the multidrug-resistant leukemia cell line CEM/ADR5000.

Table 1 — Molecular target prediction of selected flavonoids

N°	Compd	Target gene	Target description	*p* value	MTC
1	CPD5	P4HB	Protein disulfide-isomerase	1.85E-58	0.74
		ELAVL3	ELAV-like protein 3	2.77E-45	0.41
		CYP1B1	Cytochrome P450 1B1	3.69E-44	0.52
		IL2	Interleukin-2	1.74E-43	0.52
		XDH	Xanthine dehydrogenase/oxidase	1.66E-25	0.52
		ABCG2	Broad substrate specificity ATP-binding cassette transporter ABCG2	2.42E-25	0.61
		NMUR2	Neuromedin-U receptor 2	4.52E-18	0.59
		RPS6KA3	Ribosomal protein S6 kinase alpha-3	1.11E-16	0.65
		NOX4	NADPH oxidase 4	4.44E-16	0.74
		CA4	Carbonic anhydrase 4	8.88E-16	0.74
		ALOX5	Arachidonate 5-lipoxygenase	1.22E-15	0.45
		CREB1	Cyclic AMP-responsive element-binding protein 1	3.55E-15	0.29
		CA7	Carbonic anhydrase 7	3.89E-15	0.74
		PTPRS	Receptor-type tyrosine-protein phosphatase S	5.53E-13	0.36
		AKR1B1	Aldo-keto reductase family 1 member B1	2.19E-11	0.74
		TCF4	Transcription factor 4	2.40E-11	0.3
		ABCB1	ATP-dependent translocase ABCB1	6.62E-11	0.54
		CA13	Carbonic anhydrase 13	1.18E-10	0.52
		CA12	Carbonic anhydrase 12	1.58E-09	0.74
		ABCC1	Multidrug resistance-associated protein 1	9.56E-08	0.49
		TOP2A	DNA topoisomerase 2-alpha	1.02E-06	0.36
2	CPD7	CYP1B1	Cytochrome P450 1B1	5.77E-70	0.8
		ELAVL3	ELAV-like protein 3	7.07E-61	0.56
		CREB1	Cyclic AMP-responsive element-binding protein 1	3.76E-47	0.36
		P4HB	Protein disulfide-isomerase	6.45E-45	0.59
		ABCG2	Broad substrate specificity ATP-binding cassette transporter ABCG2	1.66E-36	0.73
		TCF4	Transcription factor 4	2.37E-32	0.33
		XDH	Xanthine dehydrogenase/oxidase	1.23E-30	0.8
		PTPRS	Receptor-type tyrosine-protein phosphatase S	1.94E-27	0.47
		ALOX5	Arachidonate 5-lipoxygenase	1.12E-23	0.56
		NOX4	NADPH oxidase 4	1.03E-20	0.69
		CA7	Carbonic anhydrase 7	7.63E-19	0.8
		CA13	Carbonic anhydrase 13	1.56E-18	0.4
		ABCB1	ATP-dependent translocase ABCB1	2.45E-17	0.72
		RPS6KA3	Ribosomal protein S6 kinase alpha-3	1.11E-16	0.48
		IL2	Interleukin-2	2.22E-16	0.34
		NMUR2	Neuromedin-U receptor 2	2.14E-14	0.46
		CA4	Carbonic anhydrase 4	4.08E-14	0.8
		TOP2A	DNA topoisomerase 2-alpha	1.35E-13	0.47
		ABCC1	Multidrug resistance-associated protein 1	3.47E-12	0.63
		CA12	Carbonic anhydrase 12	5.04E-09	0.8
		AKR1B1	Aldo-keto reductase family 1 member B1	1.37E-08	0.56
		AKR1B10	Aldo-keto reductase family 1 member B10	4.05E-06	0.42

The protein-protein interaction profiling, conducted using the STRING database, highlighted a robust network of interactions among the predicted molecular targets, with ABCB1, NOX4, and DAPK1 serving as central hubs due to their high connectivity (Fig. 2). This suggests that these proteins may play critical roles in modulating the cellular response to CPD5 and CPD7, particularly in overcoming multidrug resistance and inducing oxidative stress-mediated apoptosis. The biosignaling network, forecasted *via* the X2K web server, further elucidated the upstream regulatory mechanisms, identifying key kinases and transcription factors that modulate the expression of these targets. The presence of TP53 and JNK1, known regulators of the mitochondrial apoptosis pathway, aligns with the docking results of

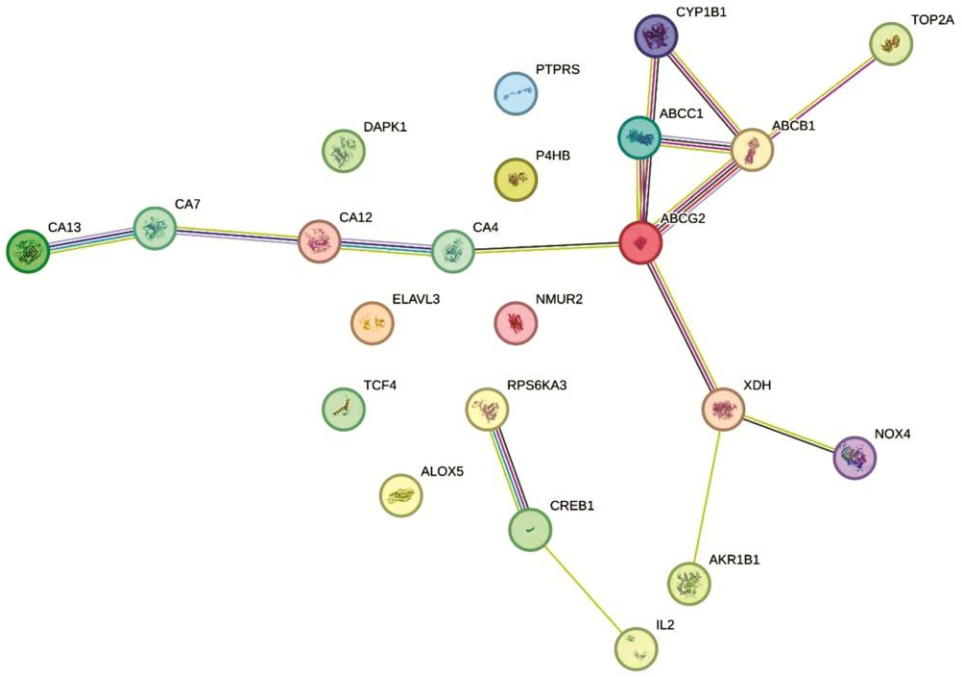

Fig. 2 — Protein-protein interactions of molecular targets of selected flavonoids.

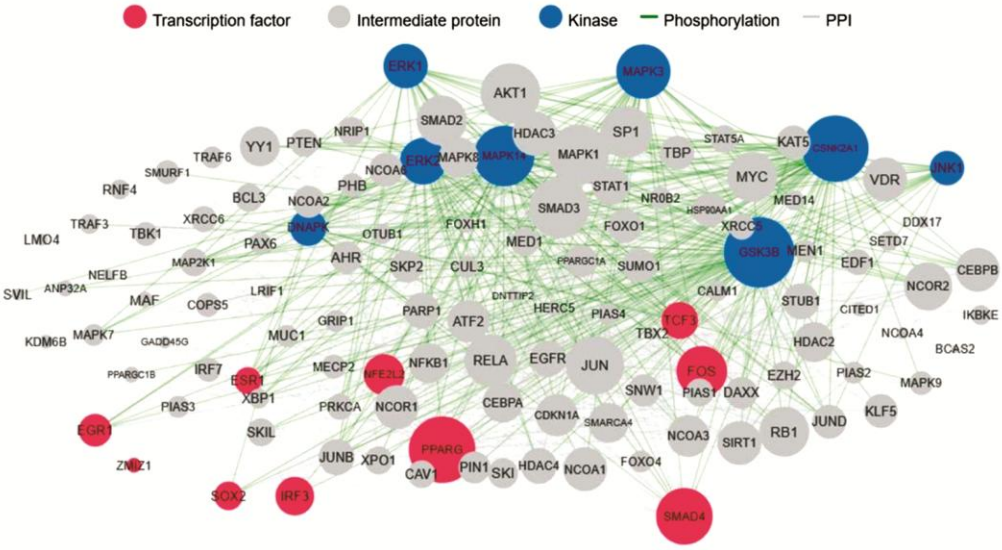

Fig. 3 — Network of kinases and transcription factors linked to molecular targets of selected flavonoids.

CPD5 and CPD7 against caspase-3, indicating a potential mechanism whereby these flavonoids induce caspase-3 activation through oxidative stress and DNA damage signaling (Fig. 3).

The pharmacological mechanism of the selected flavonoids has been elucidated through molecular target predictions, protein-protein interaction profiling, and biosignaling network analysis, providing a foundation for their docking into caspase-3. The analysis identified JNK1, a stress-activated kinase, as a key regulator implicated in apoptosis *via* the mitochondrial pathway, directly supporting the docking of flavonoids into the protein 4JJE to activate caspase-3 (Fig. 4A). NOX4 and XDH, identified as central hubs in the PPI network, generate reactive oxygen species, contributing to oxidative stress that triggers cytochrome c release and subsequent caspase-3 activation, a mechanism validated by the docking studies[21,22]. P4HB, highlighted in the molecular target predictions, is involved in endoplasmic reticulum

stress and may enhance apoptosis through the unfolded protein response, further aligning with the caspase-3 activation pathway explored *via* docking. AKT1, a survival kinase identified in the biosignaling network, may be inhibited under these stress conditions, facilitating caspase-3-mediated cell death as confirmed by the docking results[23]. Transcription factors such as TP53 and CREB1, revealed through the X2K analysis, regulate the expression of pro-apoptotic genes like BAX and PUMA, reinforcing the caspase-3 activation pathway targeted by the docking approach (Fig. 4B). Additionally, ABCB1, a pivotal protein in the PPI network and a hallmark of multidrug resistance in CEM/ADR5000, suggests that the flavonoids may overcome resistance by modulating P-glycoprotein activity, thereby enhancing intracellular accumulation of the compounds and potentiating apoptotic signaling *via* caspase-3, a hypothesis supported by the docking into 4JJE.

These findings are consistent with prior studies on flavonoid-induced apoptosis in cancer cells, where oxidative stress, transcription factor modulation, and DNA damage have been recognized as key drivers of caspase-3 activation[24,25]. The identification of TOP2A as a target, derived from the molecular target predictions, further supports the potential of these flavonoids to induce DNA damage, a known upstream trigger for caspase-3 activation in leukemia cells, which was subsequently explored through docking. However, the involvement of NFKB1, detected in the biosignaling network and known for its potential anti-apoptotic effects, indicates a complex regulatory network that may require further investigation to clarify its role in CEM/ADR5000 resistance. The integration of molecular target predictions, PPI profiling, and biosignaling network analysis has thus provided a robust framework for selecting 4JJE as a critical docking target, offering a comprehensive understanding of the therapeutic potential of selected flavonoids in inducing caspase-3-mediated apoptosis in multidrug-resistant leukemia.

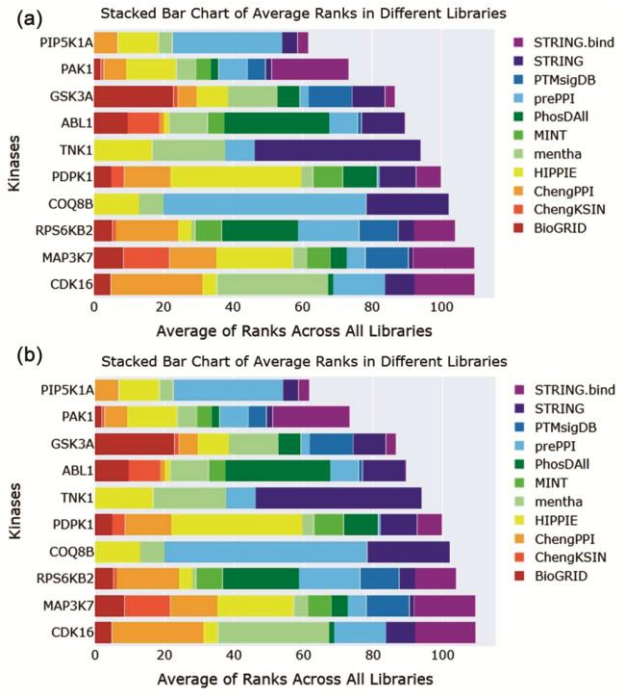

Fig. 4 — Selected flavonoids associated with kinases (A) and transcription factors (B) average rank across biological libraries.

Molecular docking analysis

Molecular docking is a powerful computational technique used as a screening tool to identify compounds that can bind to a specific site of a known protein structure. It simulates the interaction between a ligand and a protein, predicting their binding affinity, binding mode, and potential therapeutic applications[26]. Thus, this study aimed to determine the binding energy and interactions between the protein 4JJE and the selected ligands, CPD5 and CPD7, compared to the reference, Doxorubicin. The active sites of the protein, which serve as the reaction centers that attach to the ligand, elicit a biological effect, facilitate the transition to the active state, and release the products, were identified as a preliminary step before docking. Visualization of the 4JJE protein structure revealed the active sites, including Ser58, Arg64, Ser120, His121, Gly122, Gln161, Cys163, Tyr204, Ser205, Trp206, Arg207, Asn208, Ser209, Lys210, Trp214, Ser249, and Phe250 (Fig. 5).

The interactions of the selected ligands within the binding pockets of the protein 4JJE are presented in Table 2. The amino acid residues involved in these interactions and their positions within the ligand-binding site were meticulously identified. Hydrogen bonds, Van der Waals, and hydrophobic interactions between the protein and the ligands were elucidated through molecular docking, with each specific molecular interaction with the amino acids of 4JJE detailed in Fig. 6.

CPD5 exhibited interactions with the protein 4JJE through hydrogen bonds with Arg64, His121, Gly122, Gln161, Cys163, Arg207, Asn208, Ser249, Phe250, Van der Waals interactions with Ser65, Ser120, Ala162, Ser205, Trp206, Ser209, Trp214, Glu248,

Table 2 — The interactions between the docked ligands and the protein 4JJE

Docked ligands	Binding energy (kcal/mol)	Hydrogen bond interaction	Van der Waals interaction	Hydrophobic interaction
CPD5	–10.81	ARG64, HIS121, GLY122, GLN161, CYS163, ARG207, ASN208, SER249, PHE250	SER65, SER120, ALA162, SER205, TRP206, SER209, TRP214, GLU248, SER251	CYS163, ARG207
CPD7	–7.92	ARG64, SER120, ARG207	GLY122, GLN161, ALA162, LEU168, SER205, PHE256	HIS121, CYS163, TYR204, TRP206, ARG207
Doxorubicin	–8.39	SER205, ARG207, ASN208, ASP211, TRP214, PHE250	GLN217, GLU246, GLU248, SER249, SER251	TRP206, ARG207, TRP214, PHE247

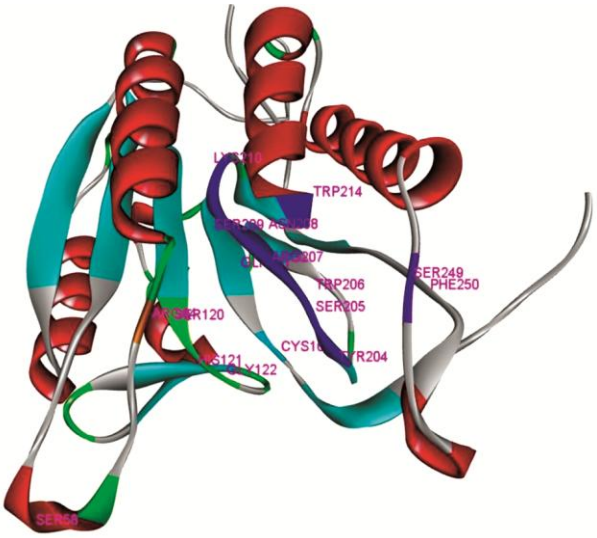

Fig. 5 — The active sites of the protein 4JJE.

Ser251, and hydrophobic interactions with Cys163, Arg207. Among these, most amino acid residues are located within the active sites of the protein 4JJE, except for Ser65, Ala162, Glu248, and Ser251 (Fig. 6A). The binding energy for CPD5 with the protein 4JJE was -10.81 kcal/mol, indicating a strong affinity.

CPD7 interacted with amino acid residues of the protein 4JJE through hydrogen bonds with Arg64, Ser120, Arg207, Van der Waals interactions with Gly122, Gln161, Ala162, Leu168, Ser205, Phe256, and hydrophobic interactions with His121, Cys163, Tyr204, Trp206, Arg207. Among these, residues Arg64, Ser120, His121, Gly122, Gln161, Cys163, Tyr204, Ser205, Trp206, Arg207 are part of the active sites of the protein 4JJE. The binding energy for CPD7 with the protein was -7.92 kcal/mol (Fig. 6B).

Doxorubicin, used as a reference compound, showed hydrogen bond interactions with Ser205, Arg207, Asn208, Asp211, Trp214, Phe250, van der Waals interactions with Gln217, Glu246, Glu248, Ser249, Ser251, and hydrophobic interactions with Trp206, Arg207, Trp214, and Phe247. Among these, amino acid residues Ser205, Trp206, Arg207, Asn208, Trp214, Ser249, Phe250 are located within the active sites of the protein 4JJE. The binding energy for Doxorubicin with caspase-3 was -8.39 kcal/mol (Fig. 6C).

All three selected compounds demonstrated hydrogen bonds, Van der Waals, and hydrophobic interactions, with hydrogen bonds and hydrophobic interactions playing an important role in stabilizing the ligand-protein complex[27]. In contrast, Van der Waals interactions contribute to high material functionality, determine the formation of the protein-ligand complex, distinguish the compound's subtle structural features, and enhance the stability of the protein complexes[28]. CPD5 exhibited the highest number of interactions (18 total, with 14 at active sites), predominantly hydrogen bonds, leading to the most negative binding energy (-10.81 kcal/mol). CPD7, with 13 interactions (10 at active sites), showed a less negative binding energy (-7.92 kcal/mol), while Doxorubicin, with 13 interactions (7 at active sites), recorded a binding energy of -8.39 kcal/mol. Notably, the more negative the binding affinity, the stronger the bond between the receptor and the ligand, suggesting greater potency[29]. Thus, CPD5 emerges as the most stable and effectively localized ligand within the protein 4JJE binding pocket, followed by Doxorubicin and CPD7. These findings lay a promising foundation for conducting molecular dynamics studies to further explore ligand dynamics within the target protein's binding site, with experiments planned for CPD5 and CPD7 compared to the reference Doxorubicin, starting from the ligand-protein complex structures derived from the docking studies.

Molecular dynamics simulation

Molecular docking and molecular dynamics simulation are complementary computational techniques in drug discovery and related fields. Docking predicts the binding pose and affinity of a

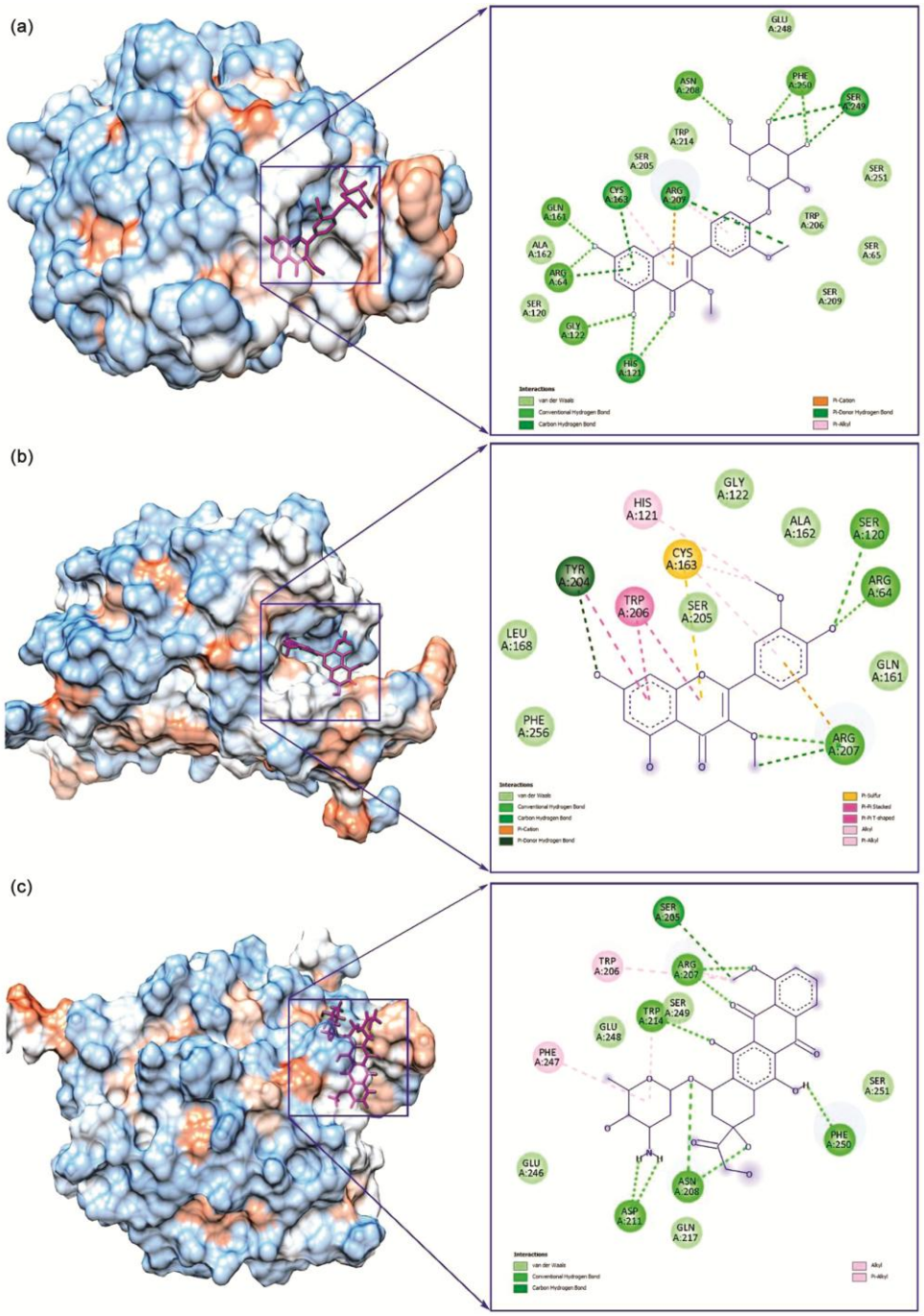

Fig. 6 — 2D and 3D interaction diagrams between 4JJE protein receptor and ligands. (A) CPD5, (B) CPD7, (C) Doxorubicin.

ligand to a receptor, while molecular dynamics simulation studies the dynamic interactions and stability of the protein-ligand complex over time[30]. The analysis examined RMSD, RMSF, Rg, and H-bonds results. The total energy was calculated as -516,437 kJ/mol for CPD5 and -517,781 kJ/mol for CPD7. The potential values were calculated as -641,723 kJ/mol for CPD5 and -643,138 kJ/mol for CPD7. The total energy and potential values for the reference Doxorubicin were -517,038 and -642,373 kJ/mol, respectively. The system was equilibrated at a temperature of 300 K.

The RMSD is a metric used to assess the structural similarity between two protein-ligand complexes, or between different conformations of a protein-ligand complex during a molecular dynamics simulation.

A lower RMSD indicates greater structural similarity. It is commonly used to evaluate the stability of a complex and the accuracy of docking simulations[31]. The RMSD values for the complexes of CPD5, CPD7, and Doxorubicin with protein 4JJE ranged from approximately 0.3 to 0.7 nm over 100 ns of simulation (Fig. 7A). This result indicates that CPD5 and Doxorubicin exhibited relatively stable structural fluctuations, with RMSD values generally fluctuating between 0.3 and 0.5 nm, suggesting a more consistent binding interaction with the protein. In contrast, the RMSD values for the CPD7-4JJE complex ranged from 0.4 to 0.7 nm, showing slightly greater structural fluctuations during the simulation. A high RMSD, particularly for CPD7, suggests larger conformational changes, which may indicate a less tight binding to the target protein, potentially affecting its stability within the binding pocket. This variability could imply that CPD7 undergoes more significant structural shifts or adaptations than CPD5 and Doxorubicin. Therefore, it can be concluded that CPD5 and Doxorubicin may maintain their original structure more effectively, with less variation, making them potentially more stable ligands for the protein 4JJE compared to CPD7.

The RMSF values in protein-ligand complexes indicate the average deviation of individual atoms from their mean positions over time. Specifically, RMSF helps quantify a protein-ligand complex's flexibility and dynamic behavior, revealing regions that are more mobile or undergo significant conformational changes during a simulation[32]. Fig. 7B demonstrates that the RMSF values of the CPD5, CPD7, and Doxorubicin complexes with the protein 4JJE are similar across residues 0-300, suggesting comparable flexibility in these regions. This flexibility may be attributed to the distance of these residues from the active binding site, which includes key residues such as Arg64, His121, and Cys163. In the case of the CPD7-4JJE complex, the RMSF values exhibited higher mobility at specific regions, particularly around residues 60-120 and 180-240, indicating that CPD7 has more mobile moieties compared to CPD5 and Doxorubicin. Thus, CPD5 and Doxorubicin display stable, less flexible structures, whereas CPD7 shows distinct mobile regions that

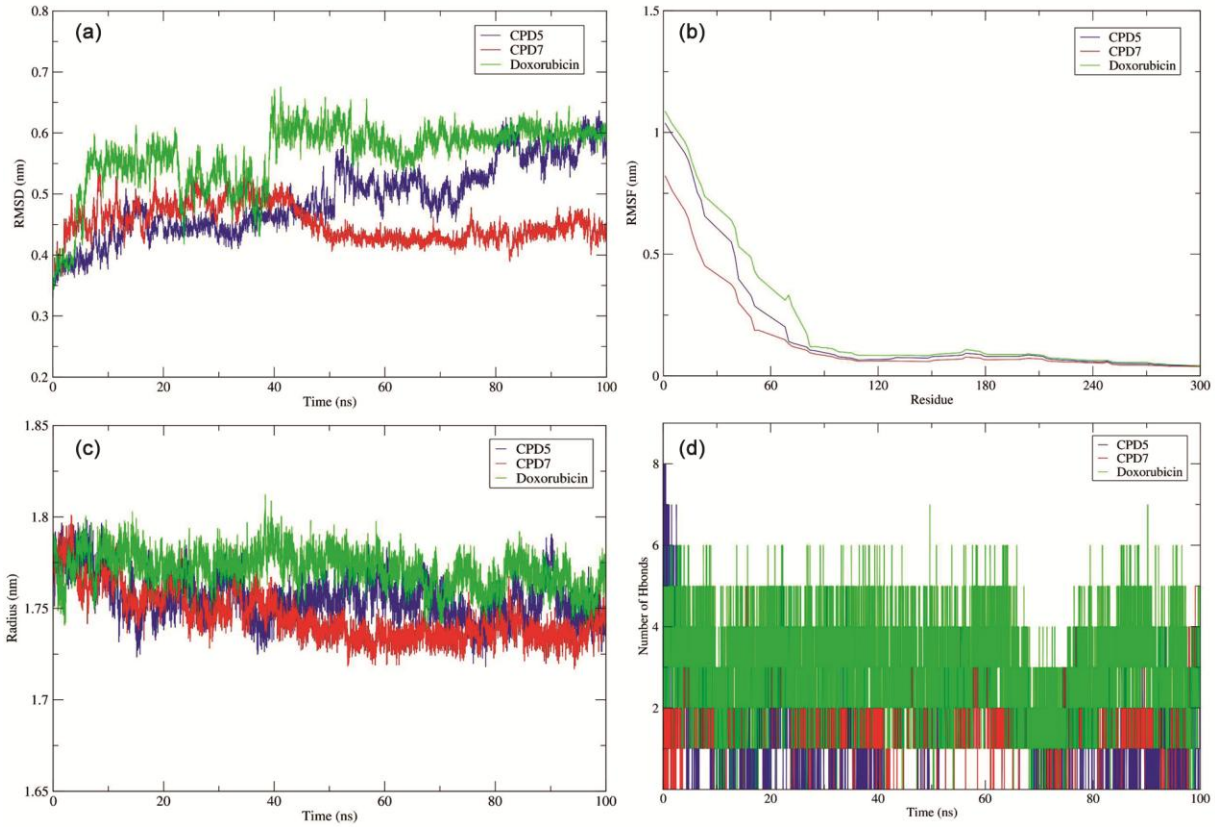

Fig. 7 — Molecular dynamics simulation results for the bindings of CPD5 (blue), CPD7 (red) and Doxorubicin (green) with 4JJE protein. (A) RMSD, (B) RMSF, (C) Rg, (D) H-bond.

may influence its interactions or stability within the binding pocket.

The Rg is a measure of the compactness of a protein, calculated as the root mean square distance of each atom from the protein's center of mass. Higher Rg values generally indicate a more unfolded or expanded protein structure, while lower Rg values suggest a more compact and folded protein state[33]. The analysis of the Rg values for each complex is shown in Fig. 7C. The Rg value represents the overall shape of the protein, with smaller values indicating a more compact structure. The Rg values for all complexes were consistently stable, ranging from 1.65 to 1.85 nm, confirming that the CPD5-4JJE, CPD7-4JJE, and Doxorubicin-4JJE complexes exhibit relatively compact protein structures.

In molecular dynamics simulations, the number of hydrogen bonds in a protein-ligand complex varies greatly depending on the specific interaction and the properties of the protein and the ligand. Hydrogen bonds are a crucial factor in binding affinity and selectivity. In general, protein-ligand complexes can have multiple hydrogen bonds, and these bonds can be strong or weak depending on their energy[34]. Hydrogen bonds were observed throughout the simulation, with the CPD5-4JJE complex maintaining 1-8 bonds and the Doxorubicin-4JJE complex sustaining 1-6 bonds, while the CPD7-4JJE complex displayed a lower range of 1-5 bonds. These results indicated that CPD5 and Doxorubicin remained within the binding pocket for the entire simulation and were stronger than CPD7 (Fig. 7), suggesting a more stable interaction with the protein 4JJE.

The molecular dynamics simulation results reveal a persistent inhibition mode and consistent binding interactions in all simulations. These findings indicate that the binding of all selected flavonoids to the protein 4JJE was stable throughout the simulation, with CPD5 and Doxorubicin demonstrating enhanced stability due to lower RMSD and RMSF fluctuations, a compact Rg profile, and a higher number of hydrogen bonds. This stability supports their potential as effective inducers of caspase-3-mediated apoptosis in multidrug-resistant leukemia (CEM/ADR5000), with CPD5 (-10.81 kcal/mol) and Doxorubicin (-8.39 kcal/mol) showing superior binding affinity compared to CPD7 (-7.92 kcal/mol). The consistent interactions observed underscore the therapeutic promise of flavonoids, warranting further investigation through extended simulations and experimental validation to optimize their efficacy.

In silico pharmacokinetics ADMET prediction

In silico methods, which use computational approaches, are increasingly used to predict the pharmacokinetic and toxicity properties of small molecules, aiding in identifying potential therapeutic candidates. These methods offer advantages like rapid predictions for large compound sets, high-throughput analysis, reducing costs, and increasing the likelihood of successful clinical trials[35]. In this study, ADMET predictions were conducted using the pkCSM databases to assess the oral bioavailability of selected compounds in comparison to Doxorubicin[36], with detailed results provided in Table 3.

Absorption is the process by which a drug moves from its administration site into the bloodstream. It is the first stage in the body's processing of a drug, also known as pharmacokinetics. CPD7 presented an intestinal absorption value higher than 84.103%, which guarantees a good absorption by the human intestine, better than the CPD5 (40.124%) and the Doxorubicin (62.372%).

In terms of distribution indicators, a volume of distribution at steady-state (VDss) value above 0.45 indicates that the drug is distributed extensively outside of the plasma, meaning it is likely found in tissues and organs[37]. The provided statement is generally considered accurate. A high blood-brain barrier (BBB) permeability, or good penetration, is often indicated when the logBB value is greater than 0.3. Conversely, a low permeability or poor penetration is typically suggested when logBB is less than -1[38]. LogPS is a measure of permeability, specifically the permeability-surface area product, and is often used to predict the ability of a drug to cross the blood-brain barrier. For the central nervous system (CNS) index, compounds with a LogPS value greater than -2 are considered to have a higher likelihood of penetrating the CNS. In contrast, compounds with a LogPS value less than -3 are likely to be unable to penetrate the CNS[39]. The distribution of a drug is evaluated through the steady-state volume of distribution (VDss). Once a drug enters the bloodstream, it is distributed throughout the body's tissues. Drug distribution refers to the movement of the drug from the bloodstream into various tissues. The steady-state volume of distribution (VDss) represents the theoretical volume required to uniformly distribute the total dose of a drug to achieve the same concentration as in blood plasma. A higher VDss value indicates greater distribution into tissues rather than plasma. A VDss value above 0.45 is

Table 3 — Predicted properties ADMET of CPD5, CPD7, and Doxorubicin

ADMET properties	Unit	CPD5	CPD7	Doxorubicin
Water Solubility	(Log mol/L)	–3.588	–3.529	–2.915
Caco2 permeability	(Log Papp in 10^{-6} cm/s)	0.53	0.637	0.457
Intestinal absorption (Human)	(% Absorbed)	40.124	84.103	62.372
Skin permeability	(Log Kp)	–2.735	–2.747	–2.735
P-glycoprotein substrate	Yes/No	Yes	Yes	Yes
P-glycoprotein I inhibitor	Yes/No	No	No	No
P-glycoprotein II inhibitor	Yes/No	No	Yes	No
VDss	(Log L/kg)	–0.07	0.173	1.647
Fraction unbound (human)	(Fu)	0.151	0.133	0.215
BBB permeability	(Log BB)	–1.966	–1.183	–1.379
CNS permeability	(Log PS)	–4.522	–3.218	–4.307
CYP2D6 substrate	Yes/No	No	No	No
CYP3A4 substrate	Yes/No	No	No	No
CYP1A2 inhibitor	Yes/No	No	Yes	No
CYP2C19 inhibitor	Yes/No	No	No	No
CYP2C9 inhibitor	Yes/No	No	No	No
CYP2D6 inhibitor	Yes/No	No	No	No
CYP3A4 inhibitor	Yes/No	No	Yes	No
Total clearance	(Log mL/min/kg)	0.732	0.687	0.987
Renal OCT2 substrate	Yes/No	No	No	No
AMES toxicity	Yes/No	No	No	No
Max. tolerated dose (human)	(Log mg/kg/day)	1.06	0.72	0.081
hERG I inhibitor	Yes/No	No	No	No
hERG II inhibitor	Yes/No	No	No	Yes
Oral rat acute toxicity (LD50)	(mol/kg)	2.473	2.275	2.408
Oral rat chronic toxicity (LOAEL)	(Log mg/kg_bw/day)	3.387	1.914	3.339
Hepatotoxicity	Yes/No	No	No	Yes
Skin sensation	Yes/No	No	No	No
Tetrahymena pyriformis toxicity	(Log ug/L)	0.285	0.337	0.285
Minnow toxicity	(Log mM)	3.454	1.401	4.412

considered high, suggesting extensive tissue distribution[20]. Table 2 shows that Harringtonine exhibited the best tissue distribution (0.701 Log L/kg), while Cephalofortine E and Fruquintinib showed very low tissue distributions (-0.25 and -0.2 Log L/kg, respectively). The standard threshold for blood-brain barrier (BBB) permeability is considered good when the value exceeds 0.3 and poor if log BB < –1 (Ref. 40). Regarding the CNS index, compounds with Log PS > -2 are deemed capable of penetrating the CNS, while those with Log PS < -3 are not considered able to penetrate the CNS[39]. The distribution indices reported by CPD7 indicated a better distribution capacity than CPD5 and Doxorubicin.

Understanding the metabolic pathways of drugs is crucial in drug development because it impacts drug efficacy, safety, and potential for drug interactions. Knowing how a drug is broken down and processed in the body helps optimize drug design, predict adverse reactions, and identify active metabolites, which can lead to new drug development or improvements. In terms of metabolism, Cytochrome P450 (CYP) enzymes are key in detoxification, facilitating the oxidation of external compounds to enhance their elimination, and are distributed across various tissues[41]. The presence of CYP inhibitors can modify drug metabolism, potentially undermining the intended therapeutic outcomes[42]. Consequently, evaluating a compound's ability to inhibit these enzymes is of paramount importance. To date, 17 CYP families have been recognized in humans, though only CYP1, CYP2, CYP3, and CYP4 contribute significantly to drug metabolism. Within these, the isoforms CYP1A2, CYP2C9, CYP2C19, CYP2D6, and CYP3A4 are responsible for metabolizing over 90% of drugs in the initial phase, with CYP2D6 and CYP3A4 playing the most dominant roles[43,44]. The metabolism of flavonoids in the liver is influenced by changes in CYP enzyme

activity, which can modulate their efficacy[45]. For this reason, we evaluated the effect of CPD5, CPD7, and Doxorubicin on CYP enzymes to predict their metabolic impact as potential drugs targeting caspase-3 in CEM/ADR5000. The results indicate that CPD5 and Doxorubicin are neither substrates nor inhibitors of CYP2D6, CYP3A4, CYP1A2, CYP2C19, CYP2C9, or CYP3A4. In contrast, CPD7 is not a substrate for any of these CYP enzymes but acts as an inhibitor of CYP1A2 and CYP3A4. This suggests that CPD5 and Doxorubicin may undergo minimal Phase I metabolism by CYP enzymes, potentially preserving their activity until Phase II modification or excretion, while CPD7's inhibitory action on CYP1A2 and CYP3A4 could influence its metabolic clearance, possibly affecting its therapeutic potential.

The rate of drug clearance during excretion plays an important role in establishing appropriate dosage levels to maintain consistent drug concentrations in the body[46]. This process primarily occurs in the liver for clearance and in the kidneys for excretion, where a reduced clearance rate suggests greater drug retention within the system. In this investigation, we assessed the excretion characteristics of CPD5, CPD7, and Doxorubicin to gauge their stability as potential therapeutic agents before elimination. The calculated clearance indices revealed values of 0.732 log mL/min/kg for CPD5, 0.687 log mL/min/kg for CPD7, and 0.987 log mL/min/kg for Doxorubicin, indicating that CPD7, with the lowest clearance, may remain in the body longer than CPD5 and Doxorubicin. This prolonged retention of CPD7 could enhance its effectiveness in triggering caspase-3-mediated apoptosis at a reduced dosage compared to CPD5 and Doxorubicin, due to its extended availability in the physiological environment.

Evaluating the toxicity of new chemical entities is a crucial aspect of drug discovery and development. It is often part of the ADMET assessment, a set of properties determining a compound's suitability as a potential drug. The AMES test, commonly used to evaluate compound toxicity[47], was applied to assess CPD5, CPD7 and Doxorubicin. The results showed that CPD5, CPD7, and Doxorubicin are all non-toxic according to the AMES test.

Based on the *in silico* ADMET evaluation results for CPD5, CPD7, and Doxorubicin, it can be concluded that CPD7 satisfies all the pharmacokinetic criteria, in which this compound is non-toxic, exhibits superior distribution capacity, and demonstrates high absorption. This study suggests that CPD7 is a promising candidate for inducing caspase-3-mediated apoptosis and a potential future drug for treating multidrug-resistant leukemia (CEM/ADR5000).

Conclusions

Based on the pharmacokinetic and molecular target analyses of CPD5, CPD7, and Doxorubicin, these compounds were successfully evaluated as potential agents for inducing apoptosis in multidrug-resistant leukemia (CEM/ADR5000). The findings demonstrated that these flavonoids are likely to promote apoptosis by modulating critical signaling pathways, activating caspase-3, and influencing cell survival and proliferation. Molecular docking analyses with the caspase-3 structure (PDB ID: 4JJE) revealed that CPD5 and Doxorubicin exhibited more stable binding energies and were better localized within the protein 4JJE compared to CPD7. The molecular dynamics simulation further validated a consistent binding mode, with stable interactions maintained throughout the simulation, highlighting their potential to effectively trigger caspase-3 activation. *In silico* ADMET predictions were also conducted to assess the oral bioavailability of the selected compounds. As a result, CPD7 meets all the pharmacokinetic criteria, being non-toxic, demonstrating superior distribution capacity, and showing high absorption. This characterization positions CPD7 as a promising future drug for treating multidrug-resistant leukemia by inducing apoptosis through caspase-3 activation.

Supplementary Information

Supplementary information is available in the website https://nopr.niscpr.res.in/handle/123456789/58776.

Funding

This research is funded by Thai Nguyen University of Education under grant number TNUE-2025-10.

Conflict of Interest

The authors declare that there are no conflicts of interest.

Author's Contributions

The author confirms the sole responsibility for the conception of the study, presented results and manuscript preparation. All data were generated in-house and that no paper mill was used.

References

1 Dallas S, Miller D S & Bendayan R, *Pharm Rev,* 58 (2006) 140.
2 Bukowski K, Kciuk M & Kontek R, *Int J Mole Sci,* 21 (2020) 3233.
3 Goel H, Kumar R, Tanwar P, Upadhyay T K, Khan F, Pandey P, Kang S, Moon M, Choi J, Choi M & Park M N, *Biomed Pharm,* 160 (2023) 114351.
4 DiNardo C D & Cortes J E, *Expert Opin Pharm,* 16 (2015) 95.
5 Elmore S, *Toxicol Path,* 35 (2007) 495.
6 D'Amelio M, Sheng M & Cecconi F, *Trends Neurosci,* 35 (2012) 700.
7 Cragg G M & Newman D J, *J Ethnopharm,* 100 (2005) 72.
8 Salmerón-Manzano E, Garrido-Cardenas J A & Manzano-Agugliaro F, *Int J Env Res Public Health,* 17 (2020) 3376.
9 Mir S A, Dar A, Hamid L, Nisar N, Malik J A, Ali T & Bader G N, *Curr Res Pharm Drug Discov,* 6 (2024) 100167.
10 Nchiozem-Ngnitedem V A, Omosa L K, Derese S, Efferth T & Spiteller M, *Phytomed Plus,* 2 (2022) 100234.
11 Vickers C J, González-Páez G E & Wolan D W, *ACS Chem Biol,* 8 (2013) 1558.
12 Keiser M J, Roth B L, Armbruster B N, Ernsberger P, Irwin J J & Shoichet B K, *Nat Biotech,* 25 (2007) 197.
13 Szklarczyk D, Gable A L, Nastou K C, Lyon D, Kirsch R, Pyysalo S, Doncheva N T, Legeay M, Fang T, Bork P & Jensen L J, *Nucleic Acids Res,* 49 (2021) D605.
14 Clarke D J, Kuleshov M V, Schilder B M, Torre D, Duffy M E, Keenan A B, Lachmann A, Feldmann A S, Gundersen G W, Silverstein M C & Wang Z, *Nucleic Acids Res,* 46 (2018) W171.
15 Nguyen H D, *Indian J Chem,* 64 (2025) 383.
16 Van Der Spoel D, Lindahl E, Hess B, Groenhof G, Mark A E & Berendsen H J, *J Comp Chem,* 26 (2005) 1701.
17 Guex N & Peitsch M C, *Electrophoresis,* 18 (1997) 2714.
18 Zoete V, Cuendet M A, Grosdidier A & Michielin O, *J Comp Chem,* 32 (2011) 2359.
19 Pettersen E F, Goddard T D, Huang C C, Couch G S, Greenblatt D M, Meng E C & Ferrin T E, *J Comp Chem,* 25 (2004) 1605.
20 Pires D E, Blundell T L & Ascher D B, *J Med Chem,* 58 (2015) 4066.
21 Gao L, Laude K & Cai H, *Vet Clin North Am Small Anim Prac,* 38 (2008) 137.
22 Chen C, Li L, Zhou H J & Min W, *Antioxidants,* 6 (2017) 42.
23 Yang X, Liu S, Kharbanda S & Stone R M, *Leuk Res,* 36 (2012) 205.
24 Jomova K, Alomar S Y, Valko R, Liska J, Nepovimova E, Kuca K & Valko M, *Chem Biol Interact,* 413 (2025) 111489.
25 Slika H, Mansour H, Wehbe N, Nasser S A, Iratni R, Nasrallah G, Shaito A, Ghaddar T, Kobeissy F & Eid A H, *Biomed Pharm,* 146 (2022) 112442.
26 Agu P C, Afiukwa C A, Orji O U, Ezeh E M, Ofoke I H, Ogbu C O, Ugwuja E I & Aja P M, *Sci Rep,* 13 (2023) 13398.
27 Patil R, Das S, Stanley A, Yadav L, Sudhakar A & Varma A K, *PLoS One,* 5 (2010) e12029.
28 Bitencourt-Ferreira G, Veit-Acosta M & de Azevedo W F, *Van der Waals Potential in Protein Complexes*, (Springer, New York) 2019, p. 79.
29 Xue Q, Liu X, Russell P, Li J, Pan W, Fu J & Zhang A, *Ecotoxic Env Saf,* 233 (2022) 113323.
30 Singh S, Bani Baker Q & Singh D B, *Molecular docking and molecular dynamics* simulation, (Academic Press, Cambridge) 2022, p. 291.
31 Reva B A, Finkelstein A V & Skolnick J, *Fold Des,* 3 (1998) 141.
32 Benson N C & Daggett V A, *J Phys Chem B,* 116 (2012) 8722.
33 Altu N S, Budiman C, Razali R, Mokhtar R A & Kamaruzaman K A, *Data,* 7 (2022) 144.
34 Alves E D, de Andrade D X, de Almeida A R & Colherinhas G, *J Mol Liq,* 349 (2022) 118165.
35 Sliwoski G, Kothiwale S, Meiler J & Lowe Jr E W, *Pharm Rev,* 66 (2014) 334.
36 Zia M, Parveen S, Shafiq N, Rashid M, Farooq A, Dauelbait M, Shahab M, Salamatullah AM, Brogi S & Bourhia M, *ACS Omega,* 9 (2024) 2161.
37 Berellini G, Springer C, Waters N J & Lombardo F, *J Med Chem,* 52 (2009) 4488.
38 Muehlbacher M, Spitzer G M, Liedl K R & Kornhuber J, *J Comp Aided Mol Des,* 25 (2011) 1095.
39 Han Y, Zhang J, Hu C Q, Zhang X, Ma B & Zhang P, *Front Pharm,* 10 (2019) 434.
40 Speciale A, Muscarà C, Molonia M S, Cimino F, Saija A & Giofrè S V, *Phyther Res,* 35 (2021) 4616.
41 Ouassaf M, Belaidi S, Khamouli S, Belaidi H & Chtita S, *Acta Chim Slov,* 68 (2021) 289.
42 Domínguez-Villa F X, Durán-Iturbide N A & Ávila-Zárraga J G, *Bioorg Chem,* 106 (2021) 104497.
43 Zanger U M & Schwab M, *Pharm Ther,* 138 (2013) 103.
44 Rodrigues-Junior V S, Villela A D, Abbadi B L, Sperotto N D, Pissinate K, Picada J N, Silva J B D, Bizarro C V, Machado P & Basso L A, *Reg Toxicol Pharm,* 111 (2020) 104553.
45 Bojić M, Kondža M, Rimac H, Benković G & Maleš Ž, *Molecules,* 24 (2019) 3174.
46 Benet L Z & Zia-Amirhosseini P, *Toxic Path,* 23 (1995) 115.
47 Ferraz E R, Umbuzeiro G A, De-Almeida G, Caloto-Oliveira A, Chequer F M, Zanoni M V, Dorta D J & Oliveira D P, *Env Toxic,* 26 (2011) 489.